PAPER

CrossMark
click for updates

A photonic crystal based sensing scheme for acetylcholine and acetylcholinesterase inhibitors

Christoph Fenzl, Christa Genslein, Alexander Zöpfl, Antje J. Baeumner and Thomas Hirsch*

We present a new scheme for sensing biomolecules by combining an enzyme hydrogel with a photonic crystal hydrogel layer that responds to ionic strength and pH changes. We demonstrate this unique combination by successfully detecting acetylcholine (ACh) and acetylcholinesterase (AChE) inhibitors. Specifically, the sandwich assembly is composed of layers of photonic crystals and a polyacrylamide hydrogel functionalized with AChE. The photonic crystal film has a red color and turns dark purple within 2–6 minutes of the enzymatic reaction upon analyte addition. This 3D photonic crystal sensor responds to acetylcholine in the 1 nM to 10 μM concentration range (which includes the relevant range of ACh concentrations in human body fluids). Michaelis–Menten kinetics of the enzyme were determined which correlated well with literature data demonstrating the uninhibited reactivity of the immobilized enzyme. Furthermore, the presence of the acetylcholinesterase inhibitor neostigmine at concentrations as low as 1 fM was demonstrated, which is even below the necessary detection limit for clinical diagnostics. We suggest that this novel concept will find its application in clinical diagnostics, for pesticide and nerve agent detection.

1 Introduction

Acetylcholine (ACh) is one of the most – if not *the* most – important neurotransmitters that plays an important role in the regulation of body processes *e.g.* as an activator of skeletal muscles.[1] In human cerebrospinal fluid the concentration of ACh is approximately 5 pmol mL^{-1}.[2] Measuring ACh concentrations in human fluids is important for diagnostic analysis and evaluation treatment effects since a lack of ACh exists in certain diseases *e.g.* Alzheimer disease. Existing tools either permit only the indirect detection of ACh or show low signal-to-noise ratios.[3,4] The enzyme acetylcholinesterase (AChE) is present at neuromuscular junctions and hydrolyses ACh.[5] Hereby ACh gets inactivated and the concentration of the transmitter is regulated at the synapses.[1,6] This mechanism can be inhibited by acetylcholinesterase inhibitors (AChEIs) and as a consequence ACh breakdown is hindered. The concentration of ACh increases, which has major effects on the parasympathetic nervous system for example reduce heart rate and muscle contractions. Persons concerned thus often die of respiratory paralysis.[7] Known inhibitors are nerve agents such as *e.g.* sarin and tabun, pesticides (*e.g.* paraoxon and parathion) and drugs (*e.g.* tacrine, donepezil and neostigmine).[8] Some of the mentioned inhibitors are lethal at low concentrations and

were used as chemical weapons. Therefore sensors for the presence of AChEI are of great importance. Gu *et al.*[9] present a dose–response assay of AChEIs based on droplet microfluidics. The authors determine the IC$_{50}$ values of carbaryl, chlorpyrifos, and tacrine by using electrochemical detection of reduced thiocholine. Saleem *et al.*[10] recently reported on inhibitor determination based on photoluminescent p-type porous silicon. The authors are capable of detecting a concentration of 1.25 μg mL^{-1} (3.7 μM) of neostigmine methyl sulfate through an increase of photoluminescence intensity at 640 nm. Neostigmine is a parasympathomimetic drug that acts as an AChEI. Concentrations in human fluids (plasma) for therapeutic indications lie in the range from 0.001 up to 0.01 μg mL^{-1}.[11] While the recent publications show great value and progress of reliable AChEI detection, the therein presented detection schemes have a number of drawbacks. The preparation, characterization, modification and readout of a porous silicon wafer are time-consuming and require especially trained personnel.[10] Further sensitivity of this approach has to be improved a 100-fold to match the relevant concentrations of neostigmine in body fluids. This limits the use in point-of-care diagnostics. From all the acetylcholinesterase inhibitors, especially the sensing of organophosphate nerve agents has been of recent interest. For example, a supramolecular sensing array based on poly-(amidoamine) dendrimers[12] has been presented for the qualitative and quantitative analysis of organophosphates in water, but no concentrations lower than 10 μM have been detected. Further, photonic crystal (PhC) sensors for these species based

Institute of Analytical Chemistry, Chemo- and Biosensors. University of Regensburg, 93040 Regensburg, Germany. E-mail: thomas.hirsch@ur.de; Fax: +49-941-9434064; Tel: +49-941-9435712

This journal is © The Royal Society of Chemistry 2015

J. Mater. Chem. B, 2015, **3**, 2089–2095 | **2089**

on acetylcholinesterase or organophosphorus hydrolase inhibition have been developed with detection limits of 4.26 fM for parathion and 0.2 μM for methyl paraoxon,[13,14] but direct immobilization of the enzyme to the PhC limits detection range and sensor versatility.

In fact, photonic crystal chemical sensors have been developed already for various analytes.[15] PhCs consist of periodically arranged structures[16,17] of a dielectric material often stabilized by a polymer.[18] They reflect light of a certain wavelength that is dependent on the angle of the incident light, the distances of particles within the structure, and the refractive indices of the structure and the surrounding medium.[19] The principle is based on Bragg's law of diffraction combined with Snell's law of reflection and can be described by the following equation where D is the center-to-center distance between particles, n_{eff} is the mean effective refractive index (RI), θ is the angle of incident light, m is the order of reflection, and λ is the wavelength of the reflected light:[20–22]

$$\sqrt{\frac{8}{3}} D \left(n_{eff}^2 - \sin^2 \theta \right)^{1/2} = m\lambda$$

The mean effective refractive index n_{eff} is defined as follows, where n_p and n_m are the refractive indices of the particles and surrounding medium, respectively, and V_p and V_m are the respective volume fractions:

$$n_{eff}^2 = n_p^2 V_p + n_m^2 V_m$$

If the initial particle to particle distance in the PhC is fixed by a polymer and the angle of incident light is kept constant, changes in the reflected wavelength will occur if the matrix swells or shrinks due to changes in D and n_{eff}.[23] This behavior can be rendered chemically selective. Since PhCs can easily be produced and their production be scaled-up, they afford a simple readout and offer label-free detection, they are highly attractive transduction systems for chemical and biosensors.[15] In contrast to intensity-based detection principles, *e.g.* fluorescence, the wavelength change contains the analytical information. This is attractive in sensor development because background noise and low signal intensity do not impede the

performance. Hence, several PhC based approaches have been described for use in chemical[18,24,25] and biological[13,14,26–29] sensing.

In this work, we present a combination of a three-dimensional photonic crystal hydrogel film with an acetylcholinesterase modified polyacrylamide gel to form a 2-layer system (Fig. 1). This arrangement responds highly selective to acetylcholine in a wide concentration range, and is also able to detect the presence of AChEI at concentrations as low as 1 fmol L^{-1}.

2 Experimental section

2.1 Materials

Acetylcholine, acetylcholinesterase, acetylthiocholine iodide (ATChI), acrylamide, 2,2-diethoxyacetophenone, 5,5′-dithiobis-2-nitrobenzoic acid (DTNB), divinylbenzene (DVB), neostigmine, sodium styrenesulfonate (NaSS), and styrene were purchased from Sigma-Aldrich (http://www.sigmaaldrich.com). Acetic acid (AA), dibutyl sebacate, dimethylsulfoxide (DMSO), methanol, N,N'-methylenebisacrylamide, and sodium hydroxide were purchased from Merck (http://www.merckgroup.com), sodium chloride from VWR (http://www.vwr.com). Sodium bicarbonate was obtained from Ferak (http://www.ferak.de), and sodium persulfate (Na$_2$S$_2$O$_8$) from Riedel-de Haen (http://www.riedeldehaen.com). The ion exchange resin (type AG-501 X8) was purchased from Bio-Rad (http://www.bio-rad.com), N,N,N',N'-tetramethylethylenediamine (TEMED) from Serva (http://www.serva.de), and tetrahydrofuran from Acros (http://www.acros.com). Styrene was freshly distilled and divinylbenzene was filtered through basic aluminum oxide before use in order to remove stabilizers.

2.2 Methods

2.2.1. Synthesis of particles. The negatively charged cross-linked polystyrene particles were synthesized as described previously by our group.[25,30] Briefly, styrene (18.8 g) and divinylbenzene (DVB; 1.2 g) were added to a volume of 152 mL of ultrapure and oxygen-purged water. The emulsion was heated to 91 °C under permanent stirring. Then, a solution of 207 mg of sodium styrenesulfonate (NaSS) in 5 mL of water was added. After 3 min, 5 mL of an aqueous initiator solution containing 29 mg of NaHCO$_3$ and 76 mg of Na$_2$S$_2$O$_8$ was injected. After additional 25 min of stirring, 10 mL of water as well as more monomers/initiator were added in the following order: (a) a mixture of 3.76 g of styrene and 240 mg of DVB, (b) a solution of 641 mg of NaSS in 5 mL of water, and (c) 5 mL of the aqueous initiator solution. After 1 h, the oil bath was removed and the mixture was allowed to cool to room temperature. The suspension was filtered through a double layer of filter paper. For purification, 50 mL of the resulting suspension of nanoparticles was centrifuged for 90 min at a relative centrifugal force (RCF) of 49 000g. The resulting sediments were suspended in 5 mL of water by vortexing and ultrasonic treatment. This procedure was repeated, and the resulting suspension was centrifuged again for 180 min (RCF 49 000g) and redispersed in 5 mL of water. The centrifuged suspension of nanoparticles was
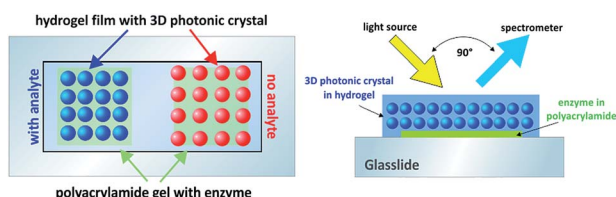

Fig. 1 The sensor consists of analyte permeable membranes assembled on a glass slide. In the presence of analyte molecules the product of the resulting enzymatic reaction – acetic acid and choline – causes shrinkage of the PhC (left) due to the change of the electrostatic environment of the system. The change in the reflected wavelength is recorded with a fiber optic spectrometer at a fixed angle of 90° to the light source (right).

diluted with 50 mL of water and the temperature of the mixture was maintained at 85 °C. After 6 days, the particles were again centrifuged according to the above protocol.

2.2.2. Determination of particle size and surface charge. A 10 μL drop of the suspension was placed on a carbon-coated copper grid. After drying, micrographs were acquired with a transmission electron microscope (TEM; type CM 12; from Philips, http://www.philips.com). Dynamic light scattering (DLS) measurements were carried out with the same suspensions using a Zetasizer Nano Series instrument (Malvern, http://www.malvern.com) operated in the backscattering mode at an angle of 173° at 25 °C after temperature equilibration for 60 s. After 20 consecutive measurements, the mean hydrodynamic radius and the polydispersity index (PDI) were extracted from the autocorrelation data.

Electrophoretic mobility of the nanospheres was measured by dispersing them at a concentration of approximately 8 g L^{-1} in a 10 mM sodium chloride solution after prolonged vortexing and sonication. Around 800 μL of the particle suspension were filled into a folded capillary cell (type DTS1060; from Malvern) and thermally held at 25 °C. Laser Doppler velocimetry with the Zetasizer nano series determined the mean electrophoretic mobility in 400 runs. The Smoluchowski model was used to calculate the ζ-potential of the dispersions.

2.2.3. Preparation of sensor films. The hydrogel-based photonic crystal layer was prepared analogous to the protocol described previously.[25,30] Briefly, acrylamide (50 mg) and N,N'-methylenebisacrylamide (2.5 mg) were dissolved in a suspension of 1 mL of poly(styrene-*co*-sodium styrenesulfonate) nanoparticles (60 g L^{-1}) in ultrapure water. A solution of 10 μL of 2,2-diethoxyacetophenone in 10 μL of DMSO and 160 mg of ion-exchange resin was added. After intense vortexing and sonication, oxygen was removed by bubbling nitrogen through the vial. The suspension was injected into a polymerization cell consisting of two microscope slides and sidewalls consisting of a Parafilm™ spacer with a thickness of 125 μm. The gel was photopolymerized by UV irradiation at 366 nm (6 W) for 5 h, after which it was fully polymerized but had not yet dried. The film was intensely washed with water. The amino groups were hydrolyzed to form carboxy groups by applying a mixture of 900 μL 1 M sodium hydroxide and 100 μL TEMED. After 6 min, the film was thoroughly washed with ultrapure water.

The enzyme gel was prepared as follows: a polyacrylamide film was prepared exactly as described above, but instead of the photonic crystal dispersion only ultrapure water was used. The transparent gel was allowed to swell in ultrapure water for 24 h. By placing the gel in a solution of 0.5 mg AChE (422 U) in 4 mL ultrapure water for 48 h, diffusion of the enzyme into the matrix was achieved. AChE was then covalently attached to the hydrogel with 1-ethyl-3-(3-dimethylaminopropyl)carboiimide (EDC) (25 mg mL^{-1}) for 1.5 h. The gel was washed several times to remove unbounded enzyme. The enzyme films were stored at 4 °C.

2.2.4. Characterization of the PhC hydrogel film. The polyacrylamide hydrogel containing the poly(styrene-*co*-sodium styrenesulfonate) nanoparticles was dried under ambient conditions and sputter-coated with gold. The morphology of the

PhC film was determined by scanning electron microscopy (SEM; type Ultra-55; from Zeiss, http://www.zeiss.com) operated at 5 kV.

2.2.5. Measurements of reflected light of the PhC-enzyme gel-assay. The enzyme gel was placed on a microscope glass slide and covered by the hydrolyzed polyacrylamide films with embedded polystyrene nanoparticles. Then, 500 μL of the analyte solutions with different concentrations were poured on the gel. The experimental arrangement to measure the reflected wavelength as a function of concentration and time consists of an illumination source, a xenon lamp (0.5 W) that was fixed at an angle of 90° with respect to the optical fiber, which was connected to an Ocean Optics USB 4000 spectrometer. The reflection spectra were recorded with Ocean Optics SpectraSuite in reflectance mode with an integration time of 100 ms per spectrum. The change of reflected light was determined as a function of time. The same procedure was used for the analysis of the PhC film alone without the enzyme gel in order to determine the PhC characteristics. All measurements were performed under ambient conditions at room temperature.

2.2.6. Measurement of the enzyme activity with Ellman's assay. A varied protocol of Ellman's assay[31] was used. Briefly, acetylthiocholine iodide (ATChI), a mimic of ACh, serves as a substrate. A solution of 35 mM ATChI in 150 mM Tris buffer (pH 8.0) was diluted in order to cover a concentration range from 1 to 6 mM. 100 μL of 10 mM 5,5′-dithiobis-2-nitrobenzoic acid were added to the respective ATChI solution to yield a total volume of 3.5 mL. Then the enzyme film was placed into the solution and the UV-visible absorbance was measured against a 150 mM Tris buffer. The absorbance at 412 nm was monitored over a 2 min time period.

3 Results and discussion

3.1 Choice of materials and sensor design

We have shown previously[25] that 3D PhCs can be prepared very efficiently *via* controlled assembly of periodic dielectric, highly charged, monodisperse polystyrene spheres. Styrene can easily be polymerized and cross-linked, and its size and low polydispersity can be well adjusted by surfactants. Styrenesulfonate functions as a secondary monomer introducing sulfonate groups providing a high surface charge. The fraction of reagents and the reaction conditions are the result of an optimization of the concentrations of the cross-linker and the initiator, and of polymerization time. Concentration, surface charge and size of the particles influence the characteristics of the PhC. Surface charges and particle diameters that are too large will lead to particle–particle distances where diffraction occurs in the IR region rather than in the visible region. If, on the other hand, surface charge and spheres are too small, the opposite can be observed and the diffracted light will come to lie in the UV region so that films will appear colorless to the eye. Generally, the particle number densities must be in the proper range for light diffraction in the visible region to occur.

Polyacrylamide (PAM) is a good choice in terms of a matrix (host) material for the polystyrene particles as well as the enzyme gel. It is well permeated by ions and all of the

components are water-soluble and transparent, so that the structural colors of the photonic crystal dispersions can be recorded without the optical influence of the hydrogel. In order to render the PhC sensitive to ionic strength and pH, the amido groups of PAM are (partially) hydrolyzed to form (anionic) carboxylate groups. That is also necessary in order to bind the enzyme covalently to the hydrogel. We have shown in an earlier study[25] that the reflected wavelength of such generated sensor films is stable between 4 and 60 °C.

The combination of an acetylcholinesterase-modified PAM hydrogel with a PhC system sensitive to ionic strength resulted in a new sandwich-type sensor (Fig. 1) for the determination of acetylcholine and the detection of AChE inhibitors. The sandwich-type arrangement enables great versatility as the selective unit of the enzyme hydrogel can deliberately be exchanged for the detection of other species. Furthermore, the color of the photonic crystal film is dependent on the electrostatic environment within. Direct immobilization of the enzyme in the PhC – as practised in existing sensors[13,14] – affects this environment and thus changes the color. By using two separate hydrogels the exact polymer composition can be chosen that best fits the user's needs without impeding the other component and thus strongly enhances versatility.

3.2 Characterization of the photonic crystal

The diameter of the polystyrene nanoparticles was determined by dynamic light scattering and transmission electron microscopy. As shown before,[25,30] the physical radius (determined by TEM) is smaller than the hydrodynamic radius (determined by DLS), as the high surface charge causes an extended hydration shell, which makes the particle appear larger in light scattering experiments. The mean diameter as calculated by evaluating 50 particles in the TEM image is 78 ± 10 nm (Fig. 2A and B), while DLS measurements showed a hydrodynamic diameter of 106 nm with a polydispersity index of 0.10. A zeta potential of -51.5 mV was calculated from the electrophoretic mobility data and proves the expected highly negative surface charge due to the presence of sulfonate groups in the polymer.

The polystyrene particles were previously shown to be stable at room temperature for over a year.[25] When assembled in the desired hydrogel, the PhC film in its native form showed a strong violet reflectance as expected which was easily seen using the spectrophotometer and the naked eye.

SEM images of the hydrogel (Fig. 2C) show that the nanoparticles are homogenously distributed and show no local aggregation in the polyacrylamide film.

3.3 Enzyme activity of the AChE film with Ellman's ATChI assay

We determined the enzyme activity with Ellman's assay. Over a 2 min time period the absorbance at 412 nm was monitored. Applying Lambert–Beer law the absorbance was converted into the reaction rate (with a molar absorption coefficient of 1.36×10^4 L mol^{-1} cm^{-1} for the p-nitrothiophenol anion at 412 nm).[32] The AChE film displays Michaelis–Menten enzyme kinetics for
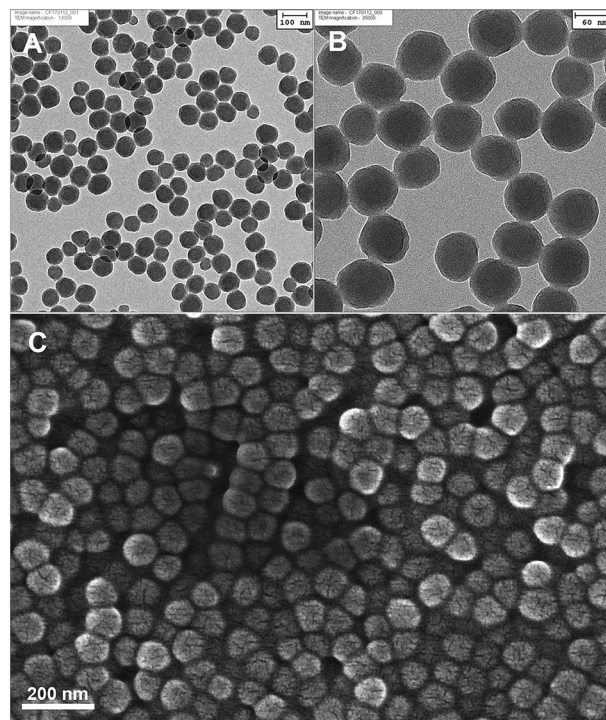

Fig. 2 (A and B) TEM images of monodisperse nanoparticles consisting of styrene, divinylbenzene and sodium styrene sulfonate. (C) SEM image of a dried photonic crystal hydrogel. Scale bars are 100 nm (A), 60 nm (B), and 200 nm (C).

the hydrolysis of ATCh indicating that 9×10^{-8} μmol min^{-1} of active AChE are attached to the hydrogel. From Lineweaver–Burk analysis the K_m was determined to be 9.8×10^{-4} mol L^{-1} and the value obtained for maximum reaction rate v_{max} was 0.11 μmol min^{-1}. The obtained K_m value agrees with those published.[33,34] The slight difference may be caused by the use of different substrates and methods or by alterations to the enzyme due to the immobilization procedure. Walker $et\ al.$[13] used the Ellman's assay to analyze the enzyme activity of a PhC based organophosphate sensor system. They incubated the film in a solution of 2000 U AChE in 4 mL 150 mM Tris buffer at pH 7.4 and determined v_{max} to be 2.4 μmol min^{-1}. The v_{max} values are in the same order of magnitude. Considering the higher amount of AChE they used, the difference in v_{max} can be explained.

3.4 Features of the PhC sensor

The enzyme cleaves ACh into acetic acid and choline and thus creating a Donnan potential. This leads to a change of the electrostatic environment of the sensor system and therefore to a blue shift of the reflected wavelength of the PhC, as the hydrogel shrinks and the particle-to-particle distances become shorter.[25] Initially the sensitivity of the PhC film towards AA (10^{-6} to 1 mol L^{-1}) was examined (Fig. 3).

The film shows a good sensitivity towards AA, $i.e.$ from 10^{-4} to 10^{-2} mol L^{-1} a shift of 150 nm of the reflected wavelength from 550 nm to 400 nm was observed.
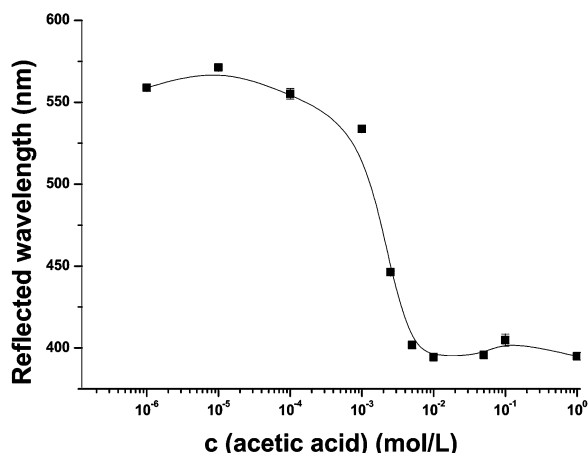
Fig. 3 Effect of solutions of acetic acid with varying concentrations on the wavelength of reflected light of the PhC film. Each data point presents the average value of five measurements; the error bars indicate the standard deviation of these measurements.

Fig. 5 Change in reflected wavelength over time after 6 minutes (reaction rate) at varying concentrations of ACh. Each data point presents the average value of five measurements; the error bars indicate the standard deviation of these measurements.

Subsequently, the reflected light was recorded over time for 16 min in order to determine the sensitivity of the sensor arrangement towards acetylcholine and to examine the overall kinetics of the PhC–enzyme gel assembly (Fig. 4).

The value at 0 min represents the reflected wavelength of the PhC film immersed in the corresponding solution before placing it on the enzyme film, whereby it is ensured that the resulting wavelength shift is only triggered by the formation of acetic acid. At increasing ACh concentrations, the reflected wavelength blue shifts. This correlates with an increasing formation of acetic acid. At a concentration of 10^{-9} M, the formation of the resulting acetic acid is too low to affect the PhC film and consequently only a slight shift of the reflected wavelength occurs. For better illustration, Fig. 5 shows the change in reflected wavelength per time after 6 min.

With increasing ACh concentration the reaction rate also increases. Employing the Michaelis–Menten enzyme kinetics model, K_m and v_{max} of the PhC–enzyme film assembly were calculated to be 6.4×10^{-9} mol L^{-1} and 5.8 nm min^{-1}, respectively. The obtained K_m value differs significantly from the values obtained without the presence of the PhC film. The fact that it is 10^5 times lower is thus explained by the added diffusion of the analyte through, in total, two different gel matrices which affects the diffusion coefficient significantly.

The linear concentration range (in the logarithmic scale) of the 3D PhC sensor system is from 10^{-9} to 10^{-5} mol L^{-1}, so the sensor could also be used for measuring ACh in body fluids, but an additional sample pre-concentration step would be advantageous, as the concentration of ACh in human beings ($\sim 5 \times 10^{-9}$ mol L^{-1})[4] is on the lower end of detectable concentrations.

Advantages of this sensing scheme are the full reversibility of the signal and the quick response. One challenge that one must always face when working with enzymes is the inactivation of the enzyme film, which in this case occurs after ten measurements. However, in real-world measurements, single-use systems that are calibrated prior to use are in any event preferred in order to avoid contamination.

In addition to the determination of acetylcholine, this 3D PhC sensor system is also able to detect smallest concentrations of an enzyme inhibitor such as neostigmine. In order to quantify the enzyme inhibition, the AChE film was immersed in solutions with 10^{-5} mol L^{-1} ACh and additionally varying concentrations of neostigmine bromide as an AChEI (Fig. 6). Neostigmine bromide itself does not influence the reflected wavelength of the PhC sensor over the whole concentration range used in these experiments.

The addition of AChEI decreases the maximum wavelength shift of reflected light. Even at the low inhibitor concentration of 10^{-15} mol L^{-1} a decrease of the maximum shift of 63 nm is observed after 16 min. This means that the final film color is no longer blue (445 nm) but green (508 nm) with the inhibitor
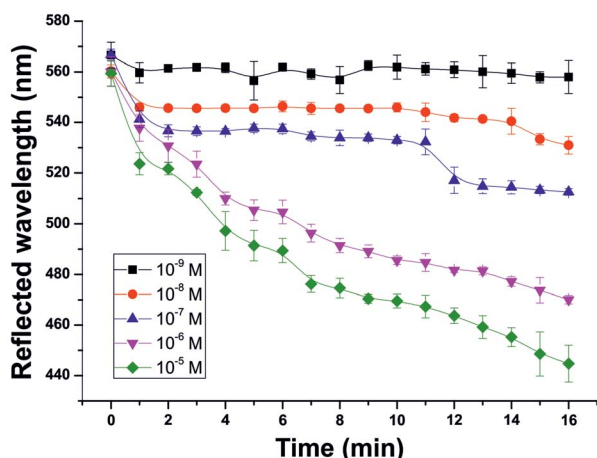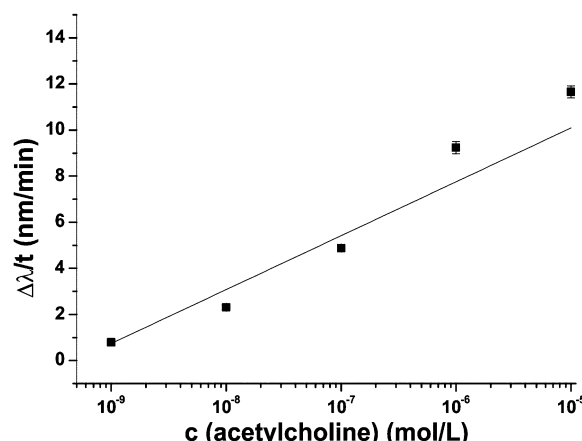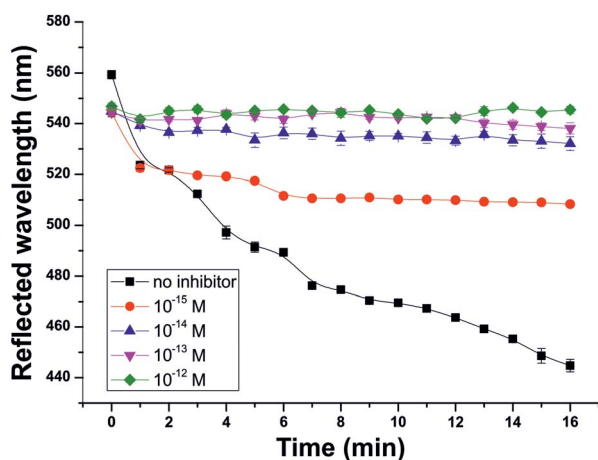

Fig. 4 Time-resolved effect of solutions of acetylcholine at varying concentrations on the reflected wavelength on the PhC–enzyme film assembly. Each data point presents the average value of five measurements; the error bars indicate the standard deviation of these measurements.

This journal is © The Royal Society of Chemistry 2015

J. Mater. Chem. B, 2015, 3, 2089–2095 | 2093

Fig. 6 Inhibition of the enzyme film with solutions of 10^{-5} M acetylcholine and varying concentrations of the inhibitor as a function of the reflected wavelength. Each data point presents the average value of five measurements; the error bars indicate the standard deviation of these measurements.

concentration as low as 10^{-15} M. Since this color change is visible to the naked eye and additionally the concentration of inhibitor in human fluids[11] is in the range of 10^{-9} to 10^{-8} mol L^{-1}, simple detection of the presence or absence of inhibitors is easily feasible. The detection limit of 1 fmol L^{-1} neostigmine is even lower than the LODs of enzyme-based PhC sensors of Asher *et al.* for parathion[13] (4.2 fmol L^{-1}) and for methyl paraoxon[14] (200 nmol L^{-1}).

4 Conclusion

We present a 2-layer approach towards optical sensing of acetylcholine and detection of an acetylcholinesterase inhibitor using photonic crystal sensor technology. The biosensor is able to detect ACh in the 10^{-9} to 10^{-5} mol L^{-1} concentration range over which a visually and instrumentally detectable wavelength shift of 70 nm is induced after just 6 min and of 115 nm after 16 min. This range also covers the concentration of ACh found in body fluids. The sensor films can be prepared from affordable materials with low production times. Aside from visual analysis, the films can be read out with a reflection spectrometer in the visible part of the spectrum. In addition, it was possible to detect the acetylcholinesterase inhibitor neostigmine at such low concentrations as 1 fmol L^{-1}, where the maximum signal change is reduced from 115 nm (without inhibitor) to 52 nm. Other features include the fast response, the lack of photobleaching, full reversibility on exposure to plain water, and inertness to changes in stability as shown in previous work.[25]

We also examined kinetics of the enzyme hydrogel film. Our results show slightly slowed substrate turnover due to diffusion processes in this hydrogel sandwich assembly.

We thus demonstrated that this biosensor is a powerful tool for the determination of ACh concentrations as well as single-use detection of AChE inhibitors most importantly enabling visual readout as well as refined instrumental quantitation. The

low-cost production and bare-eye readout possibility render this detection system suitable for test stripes. In a dip-stick format the sensor therefore lends itself nicely to point-of-care applications. While shown here using acetylcholinesterase as a model biorecognition element, the fact that the PhC-based 2-layer technology is sensitive to ionic strength/pH makes it an extremely interesting principle for a variety of bioanalytical applications including clinical analysis, for pesticide and nerve agent detection. Thus, the biosensor's principle will be adaptable to a large number of other health parameters and even to sensor arrays for multiple point-of-care diagnostics.

Acknowledgements

Notes and references

1 H. Soreq and S. Seidman, *Nat. Rev. Neurosci.*, 2001, **2**, 294–302.
2 L. Frölich, A. Dirr, M. E. Götz, W. Gsell, H. Reichmann, P. Riederer and K. Maurer, *J. Neural Transm.*, 1998, **105**, 961–973.
3 Q. T. Nguyen, L. F. Schroeder, M. Mank, A. Muller, P. Taylor, O. Griesbeck and D. Kleinfeld, *Nat. Neurosci.*, 2010, **13**, 127–132.
4 N. Ziegler, J. Bätz, U. Zabel, M. J. Lohse and C. Hoffmann, *Bioorg. Med. Chem.*, 2011, **19**, 1048–1054.
5 A. Silver, *J. Physiol.*, 1963, **169**, 386–393.
6 A. Schena and K. Johnsson, *Angew. Chem., Int. Ed.*, 2014, **53**, 1302–1305.
7 J. L. Carey, C. Dunn and R. J. Gaspari, *Respir. Physiol. Neurobiol.*, 2013, **189**, 403–410.
8 M. Pohanka, *Biomed. Pap.*, 2011, **155**, 219–223.
9 S. Gu, Y. Lu, Y. Ding, L. Li, F. Zhang and Q. Wu, *Anal. Chim. Acta*, 2013, **796**, 68–74.
10 M. Saleem, L. P. Lee and K. H. Lee, *J. Mater. Chem. B*, 2014, **2**, 6802–6808.
11 R. Regenthal, M. Krueger, C. Koeppel and R. Preiss, *J. Clin. Monit. Comput.*, 1999, **15**, 529–544.
12 Y. Liu and M. Bonizzoni, *J. Am. Chem. Soc.*, 2014, **136**, 14223–14229.
13 J. P. Walker and S. A. Asher, *Anal. Chem.*, 2005, **77**, 1596–1600.
14 J. P. Walker, K. W. Kimble and S. A. Asher, *Anal. Bioanal. Chem.*, 2007, **389**, 2115–2124.
15 C. Fenzl, T. Hirsch and O. S. Wolfbeis, *Angew. Chem., Int. Ed.*, 2014, **53**, 3318–3335.
16 G. von Freymann, V. Kitaev, B. V. Lotsch and G. A. Ozin, *Chem. Soc. Rev.*, 2013, **42**, 2528–2554.
17 S. Pal, P. M. Fauchet and B. L. Miller, *Anal. Chem.*, 2012, **84**, 8900–8908.
18 C. Fenzl, T. Hirsch and O. Wolfbeis, *Sensors*, 2012, **12**, 16954–16963.

2094 | *J. Mater. Chem. B*, 2015, **3**, 2089–2095

This journal is © The Royal Society of Chemistry 2015

19 J. D. Joannopoulos, S. G. Johnson, J. N. Winn and R. D. Meade, *Photonic Crystals: Molding the Flow of Light*, Princeton University Press, 2nd edn, 2008.

20 H. Fudouzi, *J. Colloid Interface Sci.*, 2004, **275**, 277–283.

21 Y.-J. Lee and P. v. Braun, *Adv. Mater.*, 2003, **15**, 563–566.

22 C. I. Aguirre, E. Reguera and A. Stein, *Adv. Funct. Mater.*, 2010, **20**, 2565–2578.

23 K. Lee and S. A. Asher, *J. Am. Chem. Soc.*, 2000, **122**, 9534–9537.

24 J.-T. Zhang, N. Smith and S. A. Asher, *Anal. Chem.*, 2012, **84**, 6416–6420.

25 C. Fenzl, S. Wilhelm, T. Hirsch and O. S. Wolfbeis, *ACS Appl. Mater. Interfaces*, 2013, **5**, 173–178.

26 E. Tian, J. Wang, Y. Zheng, Y. Song, L. Jiang and D. Zhu, *J. Mater. Chem.*, 2008, **18**, 1116–1122.

27 J.-H. Han, H.-J. Kim, L. Sudheendra, S. J. Gee, B. D. Hammock and I. M. Kennedy, *Anal. Chem.*, 2013, **85**, 3104–3109.

28 G. Deng, K. Xu, Y. Sun, Y. Chen, T. Zheng and J. Li, *Anal. Chem.*, 2013, **85**, 2833–2840.

29 C.-S. Huang, V. Chaudhery, A. Pokhriyal, S. George, J. Polans, M. Lu, R. Tan, R. C. Zangar and B. T. Cunningham, *Anal. Chem.*, 2012, **84**, 1126–1133.

30 C. Fenzl, M. Kirchinger, T. Hirsch and O. S. Wolfbeis, *Chemosensors*, 2014, **2**, 207–218.

31 G. L. Ellman, K. D. Courtney, V. Andres jr and R. M. Featherstone, *Biochem. Pharmacol.*, 1961, **7**, 88–95.

32 G. L. Ellman, *Arch. Biochem. Biophys.*, 1959, **82**, 70–77.

33 F. B. Hasan, S. G. Cohen and J. B. Cohen, *J. Biol. Chem.*, 1980, **255**, 3898–3904.

34 A. Ordentlich, D. Barak, C. Kronman, Y. Flashner, M. Leitner, Y. Segall, N. Ariel, S. Cohen, B. Velan and A. Shafferman, *J. Biol. Chem.*, 1993, **268**, 17083–17095.

This journal is © The Royal Society of Chemistry 2015

J. Mater. Chem. B, 2015, **3**, 2089–2095 | **2095**